

Preparation and Study of Properties of CdO: Al Thin Films Prepared by Chemical Spraying

Noor Sabah Sadeq^{1,*}, Mustafa A. Hassan¹ and Zaid G. Mohammadsalih²

¹Material Science Branch, Applied Science Department, The University of Technology, Baghdad, Iraq

²Applied Science Research Unit, Applied Science Department, The University of Technology, Baghdad, Iraq

Received: 2 Sep. 2021, Revised: 2 Nov. 2021, Accepted: 8 Dec. 2021

Published online: 1 Jan. 2022

Abstract: The studies that are related to transparent conducting oxides and the consistent motivation to improve their different characteristics have been increasingly conducted. In this work, pristine and Aluminium doped cadmium oxide, CdO: Al thin films, were synthesized by a deposition over a substrate made from glass employing spray pyrolysis technique for several Al fractions (0, 3.0, and 6.0) v/v %. The effect of Al dopant on the microstructure, morphological, optical and electrical characterisation of CdO thin films were investigated elaborately. Pure CdO and (Al: CdO) exhibited face centred cubic structure with strong peak of 200 that reflected a preferential growth. The roughness of films was increased for the samples doped with Al from (38.54 to 149.2) nm according to the increment in Al concentration. The optical analysis confirmed that the value of band gap manifested a decrement (2.5 - 2.0) eV associated with the increment in doping by Al. The measurements of Hall Effect elucidated that the CdO and Al: CdO films classified as n-type semiconductors. The range of electrical conductivity of the Al: CdO films evinced a variation from (42.4 to 35.3) $\Omega^{-1}\cdot\text{cm}^{-1}$. The results concluded from some graphs emphasized that the activation energy is equal to zero, and the Al doped CdO films became a degenerated semiconductor.

Keywords: Cadmium oxide; Aluminium; Spray pyrolysis; Scanning electron microscopy; Hall effect measurements; Optical properties.

1 Introduction

The technology of thin films is currently considered as one of the most talented fields of research. Smart windows and optical communications are among cutting edge applications related to thin films technology which made the field very promising and inspired the enthusiasm of research groups to enrich the studies associated to that field [1]. Transparent conducting oxides TCO thin films play an important role related to the aforementioned respect according to their unique optical and electrical characteristics [2]. This kind of thin films has various applications represented by optoelectronic devices, gas sensors, crystal heaters, and photovoltaic solar cells [2, 3, 4, 5, 6]. CdO, which is used as an n-type semiconductor that has a narrow direct band gap of (2.2-2.7) eV, has depicted promising horizons among TCO family due to its dual combination of high electric conductivity and high transparency [3,7, 8, 9, 10].

Several techniques can be used to fabricate CdO thin films such as spray pyrolysis [11], thermal evaporation [8] sol-gel technique [12] and chemical bath deposition [13]. Among these methods, spray pyrolysis is the most preferred technique compared to others as it permits the production of thin films at atmospheric conditions with low manufacturing cost and very low precursor materials consumption [14].

It is reported that the optical properties, electrical properties, and the band gap of CdO thin films can be modified when it is doped with small, big, or equal ionic radius to that of Cd^{+2} [15,16]. Furthermore, it is noticed that rare earth metal ions are possess a potential dopants to tune the electrical and optical characterization for the synthesized films of CdO [17]. Also, CdO metallic behaviour is entirely eliminated by doping with Al and the concentration of carriers was raised by raising the concentration of the Aluminium of the spray deposited film [18].

*Corresponding author E-mail: 100136@uotechnology.edu.iq

The present work aims to study the effect of the doping of Al with different ratios on the structure, optical, and the electrical characterization of CdO thin films and to obtain degenerated high conductive CdO thin films which can be utilized as diodes that work at high relative temperatures and as a conductive coating.

2 Experimental Sections

Chemical spray pyrolysis was employed to prepare undoped CdO and CdO: Al thin films of 3.0 and 6.0 % onto glass substrates of $(25 \times 25 \times 1.0) \text{ mm}^3$ dimensions at 400°C in an ambient atmosphere. To synthesize the undoped CdO thin films, the starting material used to prepare the precursor solutions was cadmium nitrate solution $[\text{Cd}(\text{NO}_3)_2 \cdot 4\text{H}_2\text{O}]$ of (0.2 M). This solution was prepared and sprayed over glass substrates. Aluminium nitrate solution $[(\text{Al}(\text{NO}_3)_3 \cdot 9\text{H}_2\text{O}) \text{ Al}(\text{NO}_3)_3]$ of (0.2 M) was made for synthesizing CdO: Al thin films. Different doping volume ratios of 3.0% and 6.0% were first prepared (3.0 cc per 100 ml and then 6.0 cc per 100 ml were removed from the cadmium nitrate solution, and replaced by 3.0 and 6.0 cc of aluminium nitrate, respectively). Three samples of different thicknesses were prepared for each concentration; as depicted in table 1; and a representative sample of a specific thickness from each concentration (the underlined one) was selected to carry out different measurements.

The procedure was entirely carried out at room temperature. The substrate to nozzle distance was adjusted to be 50 cm. The angle was adjusted to be 45° to perform efficient spraying. The spray time period was 4 sec. Filtered and compressed air were adjusted at a pressure of 6 kg/cm^2 .

The following mathematical facts are important to conclude the time required for deposition; table 1 displays the final deposition rate for the pure CdO and CdO: Al.

An hour = 3600 sec. Spray time period (per 1 spray) = 4 sec. Stoppage time = 30 sec.

Number of sprayings = $3600/34 = 106$

Full spraying time = $106 * 4 = 424$ sec.

Deposition rate = Thickness (average) / time (values mentioned in table 1 below).

As shown in table 1, deposition rate is going higher associated with the increment of doping ratio. Figure 1 reveals the increment of deposition rate as a function of doping ratio.

Table 1: The final deposition rate for undoped CdO and CdO: Al of different concentrations.

doping ratio %	d1 (nm)	d2 (nm)	d3 (nm)	d av. (nm)	deposition time (s)	deposition rate (nm/s)
0	<u>221.66</u>	378.45	221.65	273.92	424	0.64
3.0	254.09	324.40	<u>270.44</u>	282.97	424	0.66
6.0	475.75	243.27	<u>243.28</u>	320.76	424	0.75

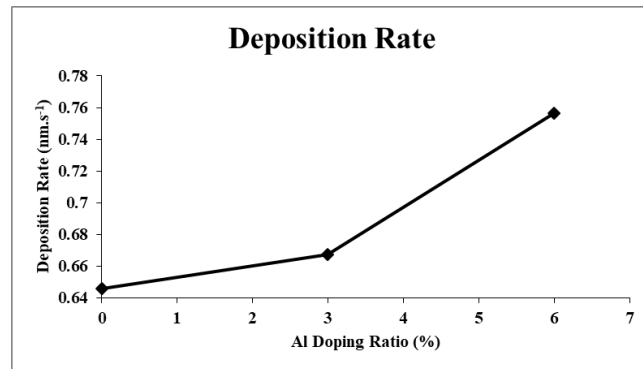


Fig. 1: The increment of deposition rate associated with the increment of doping ratio.

Glass substrates were cleaned very well using distilled water and ethanol. The temperature of the glass substrate surface was controlled by a thermocouple which was connected to be a digital temperature controller with an accuracy variation of $\pm 10^\circ \text{C}$. The microstructure, the morphology, optical, and electrical properties analyses related to the all prepared films were studied by (Philips-pw 1730, Holland) X-ray diffractometer, Atomic force microscope (AFM- Bruker-icon, America) and (T80+ UV/VIS spectrometer, PG instrument Ltd. UV/vis, PL (Avaspec 2048 TEC, Holland/Avantes). The thickness of films was measured by cross-section scanning electron microscope images (TESCAN MIRA3, Czech Republic). The operating voltage was 10 Kv.

3 Results and Discussion

3.1 Structural Characterization

The diffraction spectra (XRD) of the CdO and CdO: Al thin films are presented in Figure 2. The All synthesized films are possess a polycrystalline nature with cubic structure. During the XRD analysis, the following peaks were identified (111), (200), (220) and (311). The obtained diffraction peaks are coincide with (78-0653) JCPDS standard data [19].

Two main peaks of (200) and (111) can be noticed for all the prepared films. However, the strong intensity of the

(200) peak confirmed the preferred orientation along (002) plane with c-axis perpendicular to the substrate surface of all thin films. A unique fact can be highlighted by XRD pattern is that all films exhibited a clearly preferred orientation with (200) plane which is considerably increased with the increase of Al concentration. The increment in Al concentration leads to a shift in the preferred growth orientation from (111) to (200) plane. For FCC crystal structure, the density of atoms is the highest for the (200) orientation plane.

These outcomes confirm that the preferred plane of films is affected by the dopants and doping concentration. This result has been observed by some co-workers [20].

The work reported by the literature has confirmed the aforementioned findings represented by the preferred orientation which can be possibly changed from (111) to (200) depending on the deposition techniques of spray pyrolysis. This technique is strongly affecting both the growth kinetics and the nucleation [17].

The Scherrer's formula was used to compute the size of crystallite (D) as the following [21]:

$$D = \frac{0.94\lambda}{\beta \cos \theta} \quad (1)$$

Where, D is the grain size, λ is the x-ray wavelength, β is the full width at half-maximum (FWHM) of diffraction peaks, and θ is the Bragg angle. As presented in Table 2, the grain size decreased from 29.1 nm to 27.4 nm after doping with 3.0 % Al, and then it is marginally increased to 28.5 nm. It can be emphasized that the alteration in crystallite size is not intimately associated with the content of Al. As a result, a conclusion can be drawn that the Al concentration does not play a major role regarding the achieved outcome.

Many physical variables have a significant effect on crystallite size, such as atmosphere, growth, spray rate, concentration, and temperature of the substrate. Consequently, dopant concentration cannot be directly correlated to the crystallite size [22].

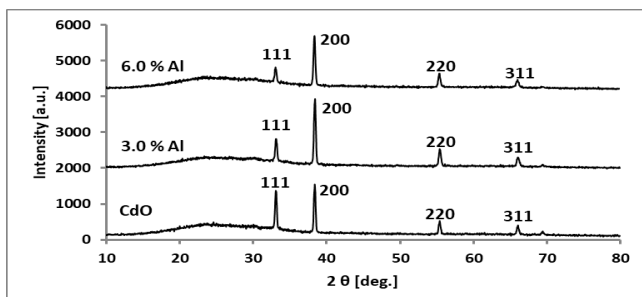


Fig. 2: XRD styles for the thin films of CdO and Al: CdO of (3.0 and 6.0) %.

Table 2. XRD (crystallite size) data for CdO films

Samples	hkl	FWHM (deg)	2 θ (deg)	Crystallite size [nm]
Undoped CdO	111	0.281	33	29.4
Undoped CdO	200	0.289	38	29.1
CdO :Al 3.0%	111	0.31	33	26.7
CdO :Al 3.0%	200	0.306	38	27.4
CdO: Al 6.0%	111	0.279	33	29.7
CdO :Al 6.0%	200	0.295	38	28.5

3.2 AFM Analysis

The roughness of undoped CdO and CdO: Al thin films were analysed by Atomic force microscopy (AFM). Three dimensional (3D) surface microstructures of CdO and Al doped CdO thin films with different Al doping concentration are shown in Figure 3. (Scan area of $5\mu\text{m} \times 5\mu\text{m}$). The root mean square roughness (R_{rms}) for undoped CdO is approximately 47.38 nm. The Al: CdO of 3.0 % and 6.0 % indicated a slightly agglomerated pyramidal shaped grains growth mode of 57.09 nm and 111.9 nm, respectively.

AFM analysis evinced that the increment in Al doping ratio produces change in the surface structure. The surfaces of films reveal a considerable roughness, and such roughness increases as the fraction of doping agent (Al) go higher. Furthermore, large pyramidal shaped particles are formed on the surfaces associated to Al concentration of 6.0 %. These results are in line with findings reported previously in the literature [23].

A research group [24] reported that the variation in the surface morphology is intimately associated with the increment in Al concentration. They also confirmed that the increment in surface roughness was obtained upon doping by 1.0 wt. % compared to that obtained upon doping by 0.5 wt. %. In addition, the same co-workers [24] concluded that the light coloured areas related to the AFM graph represented an agglomeration of grains. For the white areas, they analysed that clusters that were formed as neighbouring grains can combine with each other.

The increment in surface roughness with the raising of Al concentration is related to the increment in the films grain size. One can conclude that the mean surface roughness of the CdO thin films is evaluated as a result of the modification via the concentration of Al in these films.

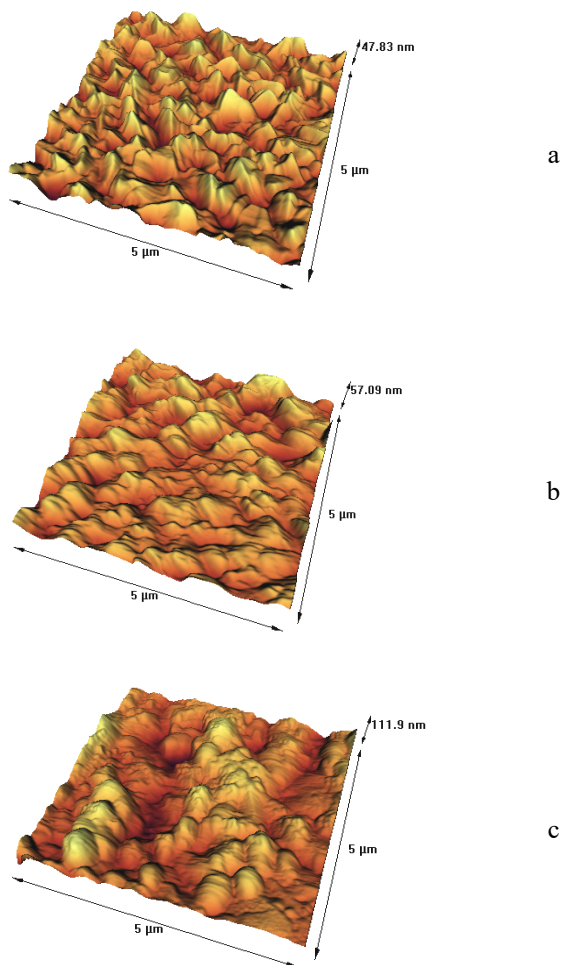


Fig. 3: AFM images of undoped CdO thin film and an Al-Doped CdO films: a) undoped CdO film, b) CdO: Al film of 3.0%, c) CdO: Al film of 6.0%.

3.3 FESEM Results

The cross-section of CdO thin films determined from the analysis of field emission scanning electron microscopy FE-SEM is shown in Figure 4. It was noticed that the grains form aggregates with different dimensions. The largest particles (that have an average of 270 nm) were obtained in the sample doped with 6.0%; meanwhile the smallest (221 nm average) were located with undoped films. It is a clear evident that the grain size rose with the increment of Al content in CdO. Figure 5a shows the micrographs of undoped CdO thin film, which comprises regular dispersed pyramidal formed particles collected with certain tiny patches. Figures 5(b-c) reveals the surface morphology of the doped CdO with 3.0% and 6.0% of Al concentration, respectively. Ameliorated grain size (pyramidal particles is clearly increased) was observed in the films doped with 3.0% of Al content. Interestingly, after doping 6.0% Al, the film morphology was changed comprising comparatively slight grains size, and lengthened pyramidal (needle)

formed particles and agglomeration were developed. The surface of film is compact and homogenous, also the size of grain is significantly increased, as illustrated in figure 5i. The foregoing discussion obviously indicates that the surface morphology of CdO thin films is effectively changing by Al – doping. The doping with Al leads to destroy the uniformity which was contributed in changing the morphology of the films represented by undefined smaller grain size, and more cracks appeared as the doping concentration of Al increased to 6.0%. As the doping ratio is going higher, the particle size is increased. This behaviour can be attributed to the almost 23% difference in ionic radius between cadmium (0.074 nm) and aluminium (0.057 nm) that observed by some collaborators [25].

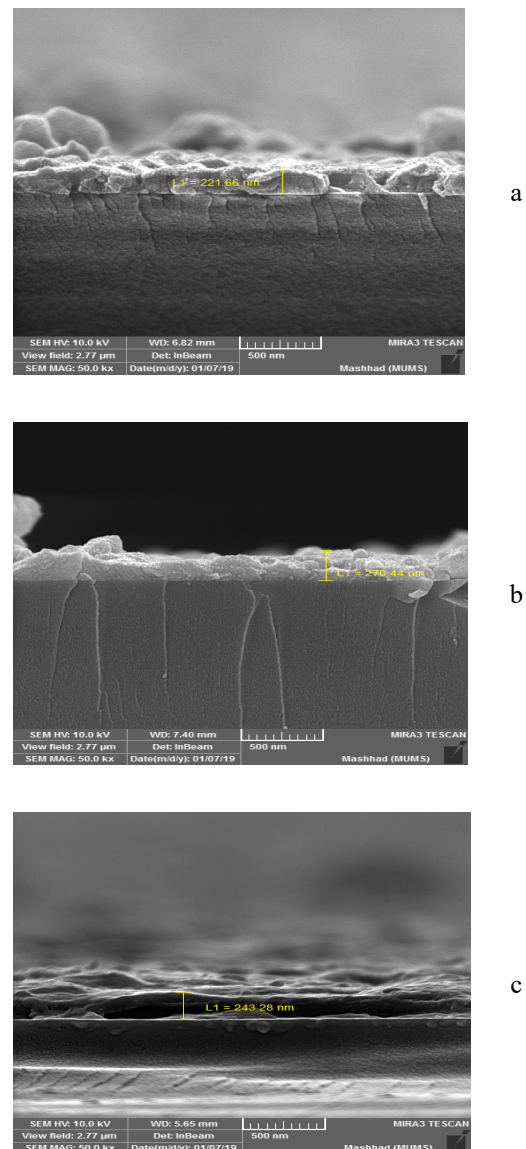
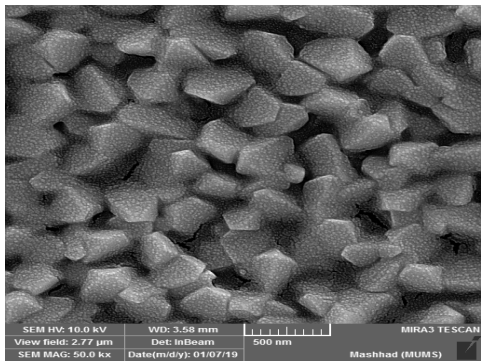
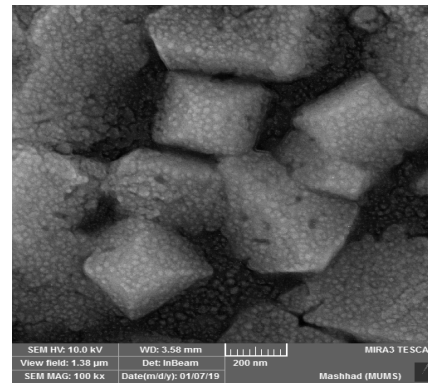


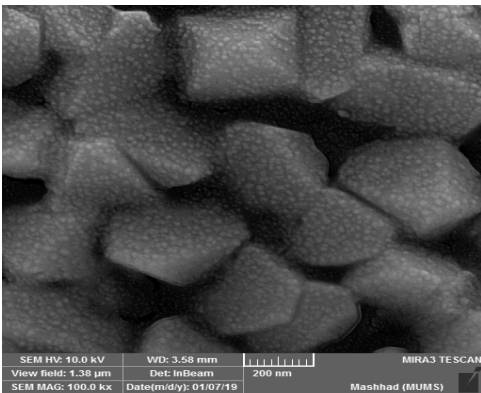
Fig. 4: SEM cross section images of thickness for (a) undoped CdO, (b, c) CdO: Al of (3.0 and 6.0) %, respectively.



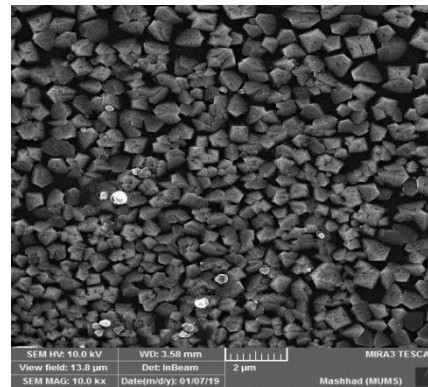
a



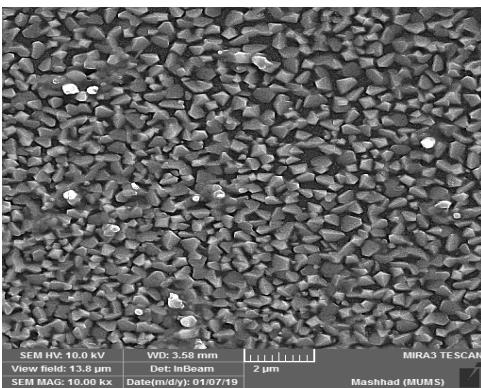
e



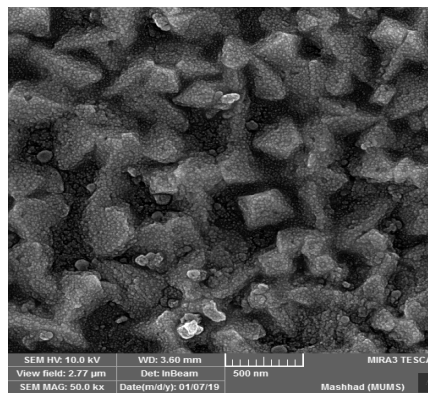
b



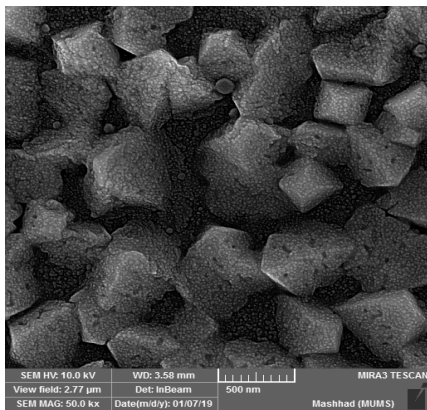
f



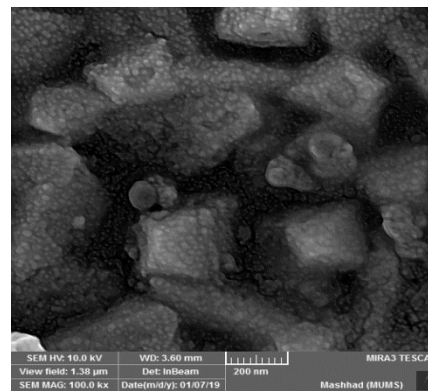
c



g



d



h

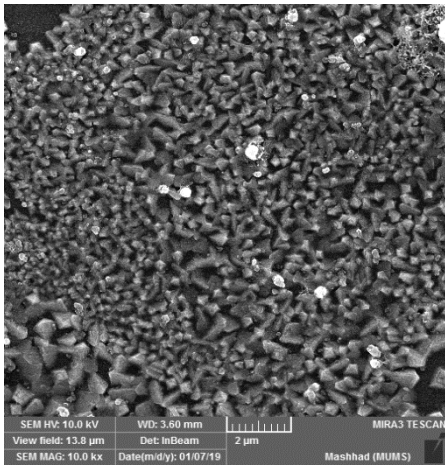


Fig. 5: FESEM images of undoped CdO films and CdO: Al. (a, b, c) undoped CdO film, (d,e,f) CdO: Al of 3.0%, and (g,h,i) CdO: Al of 6.0%.

3.4 Optical Properties

The optical band gap, E_g , can be determined from the following formula [26]:

$$h\nu = A \frac{(h\nu - E_g)^n}{2} \quad (2)$$

Where h is Plank constant, ν is the frequency, A is a constant, $h\nu$ is the photon energy, and n is a constant that relies upon the transition type ($n = 0.5$ for indirect and $n=2$ for direct). CdO represents the n -type degenerate direct band gap semiconductors [27].

Figure 6 exhibits the absorption coefficient with different Al concentrations. The former decreased as the latter is increased at short wavelengths. This outcome can be ascribed to the formation of Al oxide which has a relatively high energy gap. Consequently, at low energy (below than 2.5 eV), the undoped CdO has the lowest absorption coefficient, whereas, CdO: Al of 6.0% has the highest absorption coefficient. This behaviour may be attributed to the absorption by the local energy states (tails) inside the energy gap caused by doping.

It can be noticed that the absorption coefficient of pure CdO has a sharper bending curve than the doped CdO films which can be ascribed to the existence of tails.

The current study manifests that the E_g of (pristine CdO, 3.0 and 6.0 v/v. %) of Al doping ratio is (2.5, 2.25, 2.0) eV, respectively. The decrement in E_g for the doped CdO films could be connected to the structure modifications. The structural distortion within the CdO: Al is relatively attributed to the substitutional or interstitial replacement of Cd ions in the CdO lattice by Al ions. As a result, the CdO

structural integrity may be decreased with the Al incorporation which leads to enhance the disorder in the material. Such disorder is probably causing the band tailing influences decreasing the CdO band gap as the content of Al raises. The similar tendency related to the results of E_g for Al-doped CdO films was reported in the literature [30].

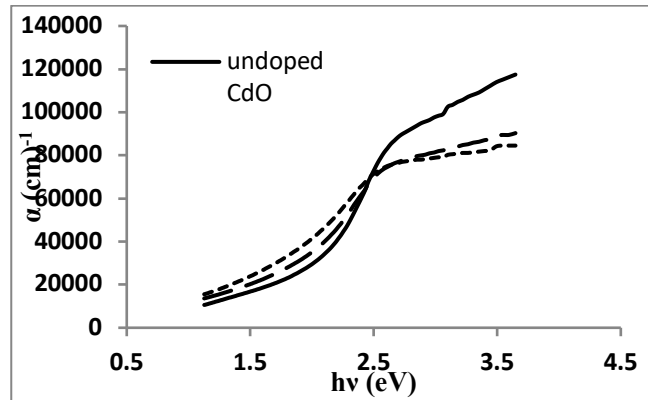
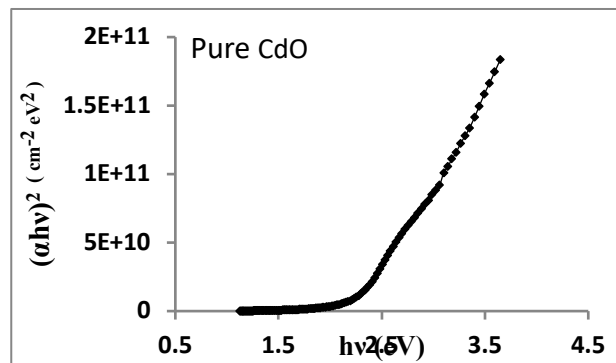
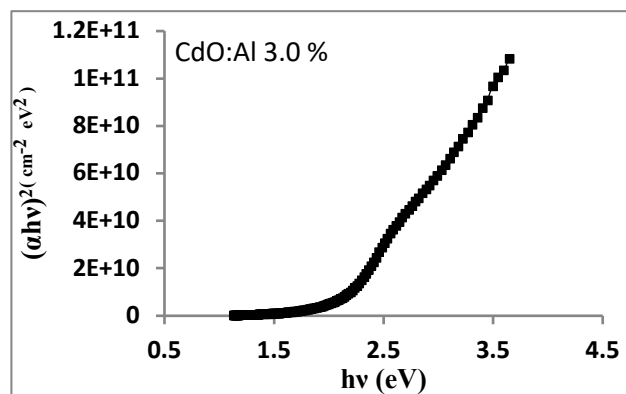


Fig. 6: The absorption coefficient for the films of pristine CdO and CdO: Al.



a



b

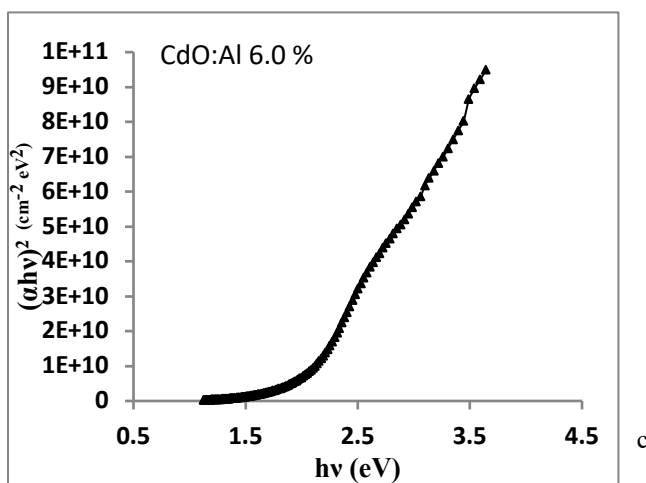


Fig. 7: Variation of E_g in samples with: (a) undoped CdO, (b) CdO: Al 3.0%, and (c) CdO: Al 6.0% thin films.

The incorporation of Al into CdO can create certain flaws in E_g of the films, and such flaws turn out the localized conditions in E_g .

The flaws concentration is associated to the localized conditions density. The Al element may perform changes in the localized conditions that lead to form overlaps. Such overlaps produce a decrement in the values of E_g . It is clear that the curvature of the graph decreases by increasing the doping ratio, and this indicates the presence of tails.

3.5. Photoluminescence

The photoluminescence (PL) spectra can be employed for determining the semiconductors band gap that takes place between the conditions at the bottom of the conduction band and the top of valence band. Figure 8 illustrates the PL spectra of pristine CdO and CdO: Al. Every single film almost exhibits the same emission and has one distinct peak centred on 651 nm and being symmetrical. The PL energies are (1.904762, 1.904762 and 1.9033) eV for (0, 3.0, and 6.0) v/v. % of CdO: Al films, respectively. These findings are ascribed to the combination of electrons and holes from the conduction band and the valence band. Moreover, it is noted that the emission of intensity of the CdO: Al of 6.0% is greater than that of pristine CdO, and the broad band observed is (625 - 680 nm) in photoluminescence peak. This may be owing to the transitions between oxygen vacancies or between Cd interstitials acting as shallow donors and Cd vacancies acting as deep acceptors [31]. The attribution of the aforementioned fact is related to the increment in defects (flaws) according to the introduction of higher ionic radii dopants which cause a lattice distortion in the host cadmium oxide. This illation is quite similar to what has been achieved in XRD section for the current study.

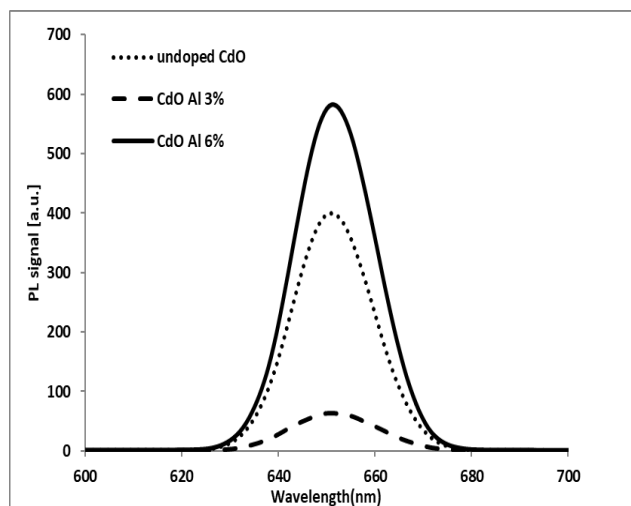


Fig. 8: PL spectra for pure CdO and CdO: Al (3.0 and 6.0) % films.

3.6 Electrical Analysis

Hall mobility, the electrical conductivity, and carrier concentration of pure CdO and CdO: Al thin films were evaluated and displayed in Figure 8, and these results are listed in Table 3.

Table 3: Electrical parameter of undoped CdO and CdO: Al films.

Sample	Mobility ($\text{cm}^2/\text{V} \cdot \text{s}^{-1}$)	n (cm^{-3})	Conductivity ($\Omega^{-1} \cdot \text{cm}^{-1}$)
Undoped CdO	4	5.00×10^{18}	3.38
CdO: Al 3.0%	10	2.00×10^{19}	42.4
CdO: Al 6.0%	2	1.00×10^{20}	35.3

The electric conductivity improved with the increment of Al concentration as a result of increasing of the carrier concentration (n). The increment of (n) is related to the abundance of production of free electrons in doped films which are from the donor sites related with the oxygen deficiencies, the interstitials of metals, and the substitution of impurities [15].

The carrier mobility of the CdO thin films is raised with the doping of Al concentration of 3.0 % to 10 ($\text{cm}^2/\text{V} \cdot \text{s}^{-1}$). This outcome is confirmed by SEM images that manifested

an expansion of pyramid structures with the doping by 3.0% of Al which reflects the fact that the mean free path has become longer. On the other hand, the carrier mobility has decreased considerably with the doping by 6.0% of Al which can be linked with SEM images that showed small and sharp pyramid structures which lead to a conclusion of a shorter mean free path, i.e. a decrement in the carrier mobility [31].

The negative sign of Hall constant approves the n-type conductivity. In addition, the increment in the Al doping ratio leads to an increment in charge carriers (electrons) which consequently lead to an improvement in electrical conductivity.

The possible explanation for the improvement in electrical conductivity is that the free charge carriers are increased in line with greater doping by Al. This behaviour can be attributed to the presence of another free electron for Al^{3+} compared to Cd^{2+} . There is a high possibility that Al occupies the sites related to Cd, or Al replaces Cd atom. At any case, Al behaves as a donor which explains the reason behind the high conductivity.

On the other hand, as Al doping is going higher, the crystalline structure might be destroyed which is consequently lead to generate capture sites for free electrons and finally leads to a lower electrical conductivity at high Al concentration [32].

The literature was showed [33] that ZnO films doped with Al evinced an increment in mobility, carrier concentration, and electrical conductivity associated with the increment of Al concentration which satisfies with what has been achieved in the current work.

In the present work, it can be observe from figure 9 the increase in the conductivity of the dopant films with 6.0% of Al in spite of a decrement in mobility that is owing to the disproportionate increment of carrier concentration that pursues the free electrons released by the vacancies of oxygen. These results agree with the outcome obtained by other collaborators [34] who reported that the electrical conductivity of the pure CdO film deposited by sol gel method was $0.5 \times 10^3 \Omega^{-1} \cdot \text{cm}^{-1}$. By doping with Al, the conductivity was increased and revealed $1.5 \times 10^3 \Omega^{-1} \cdot \text{cm}^{-1}$. In addition, the mobility of films decreased from (250 to 35) $\text{cm}^2 \text{V}^{-1} \text{s}^{-1}$ as the Al concentration was increased.

By measuring the resistivity as a function of temperature, it can be seen in figure 10 that the electrical resistivity of film decreases with an increase in Al content. These findings agree with the findings reported by some researchers [35], which depicted that the electrical resistivity decreased as the Al content increased until 5.0%. They confirmed some electrical parameters, such as resistivity, carrier

concentration, and mobility of CdO doping with Al films are sensitive to the amount of doping ratio.

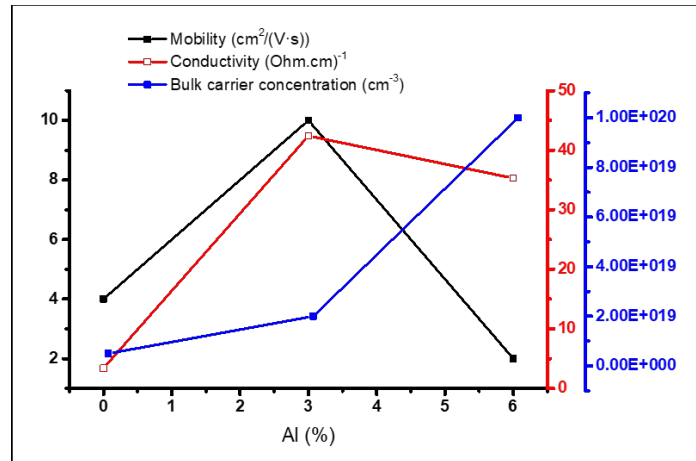


Fig. 9: The Variation in Hall mobility, carrier concentration, and CdO thin films conductivity as a function of Al doping concentration.

The direct current DC results showed that the doping leads to an improvement in conductivity as well as a change in behaviour. The undoped films exhibited an increment in conductivity by the increment of temperature beyond 375K which represents a behaviour of semiconductors. On the other hand, the doped films are irresponsive to the increment of temperature. This is because the doping ratio leads the Fermi level access to a conductive band. Figure 11 displays the graph between $\text{Ln } \sigma$ and $1000/T$. It shows that $\text{Ln } \sigma$ does not change, which means that the slope is approaching zero and consequently the activation energy is equal to zero, and the Al doped CdO films became a degenerated semiconductor. As a result, the cost effectiveness is reached by preparing the low cost doped films of CdO: Al which can be utilized as conductive coatings and can replace the indium tin oxide ITO films that have high cost.

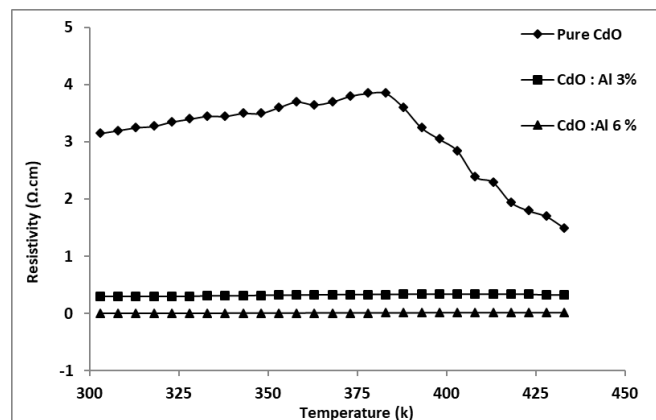


Fig. 10: The Variation in resistivity of the CdO thin films as a function of the Al doping concentration.

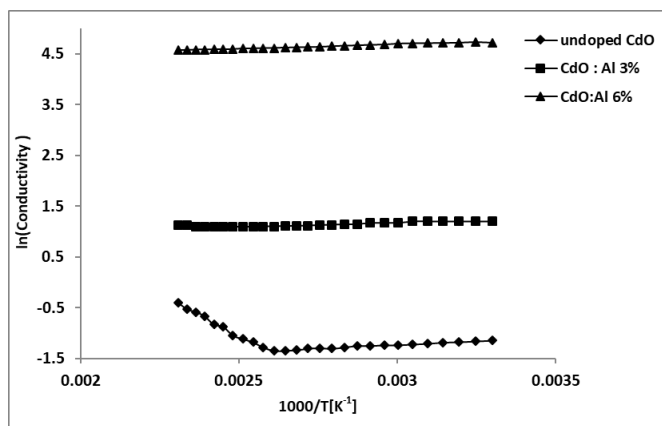


Fig. 11: The DC conductivity is showing the behaviour of ($\ln \sigma$) verses ($1000/T$).

4 Conclusions

Pure CdO and Al: CdO thin films were prepared by low cost effective spray pyrolysis method, and their characterisations were studied as a function of Al doping concentration. The different doping levels of Al have affected the structure, morphological, optical, and electrical properties of the CdO films. The films have a low absorption coefficient with a high electric conductivity. Al doped CdO films were degenerated semiconductors which means that the Fermi level access to conductive band and activation energy is zero. The Al doped CdO can be used as diodes that work in high relative temperatures and a conductive coating or based instead of FTO as well.

Acknowledgments

The authors would like to express their gratitude to Dr. Ameer Faisal, the Assistant Professor at the department of Physics, College of Science, Baghdad University for his kind help in accomplishing the required scientific measurements related to this work.

References

- [1] N. Wongcharoen, T. Gaewdang, T. Wongcharoen. Electrical properties of Al-doped CdO thin films prepared by thermal evaporation in vacuum, *Energy Procedia.*, 361–370 (2012).
- [2] B.J. Zheng, J.S. Lian, Q. Jiang. Optical and electrical properties of Sn-doped CdO thin films obtained by pulse laser deposition. *Vacuum.*, 5, 861–865 (2011).
- [3] A. Purohit, S. Chander, M.S. Dhaka. Impact of annealing on physical properties of e-beam evaporated polycrystalline CdO thin films for optoelectronic applications. *Optical Materials.*, 66, 512–518 (2017).
- [4] Rajput J K, Pathak T K, Kumar V, Swart H C, Purohit L P. Tailoring and optimization of optical properties of CdO thin films for gas sensing applications. *Physica B: Condensed*

Matte., 535, 314–318 (2018).

- [5] B.J. Zheng, J.S. Lian, Q. Jiang. Optical and electrical properties of In-doped CdO thin films fabricated by pulse laser deposition. *Applied Surface Science.*, 256, 2910–2914 (2010).
- [6] Azizar Rahman, M. Khan, M.K.R. Effect of annealing temperature on structural, electrical and optical properties of spray pyrolytic nanocrystalline CdO thin films. *Materials Science in Semiconductor Processing.*, 24, 26–33 (2014).
- [7] S. Duman, G. Turgut, B. Gurbulak. The synthesis and characterization of sol-gel spin coated CdO thin films: As a function of solution molarity. *Materials Letters.*, 126, 232–235 (2014).
- [8] M. Zaien, N.M. Ahmed, Hassan. Effects of annealing on the optical and electrical properties of CdO thin films prepared by thermal evaporation. *Materials Letters.*, 105, 84–86 (2013).
- [9] R.K. Gupta, K. Ghosh, R. Patel, P.K. Kahol. Low temperature processed highly conducting, transparent, and wide bandgap Gd doped CdO thin films for transparent electronics. *Journal of Alloys and Compounds.*, 509, 4146–4149 (2011).
- [10] A.A.Dakhel. Optical and electrical properties of copper-doped nano-crystallite CdO thin films. *Solid State Sciences.*, 31, 1–7 (2014).
- [11] P. Velusamy, R. Ramesh Babu, K. Ramamurthi, E. Elangovan, and J. Viegas. Effect of La doping on the structural, optical and electrical properties of spray pyrolytically deposited CdO thin films. *Journal of Alloys and Compounds.*, 708, 804–812 (2017).
- [12] Carballeda Galicia D M, Castanedo Perez R, Jimenez Sandoval O, Jimenez Sandoval S, Torres Delgado G, Zuniga Romero C I. High Transmittance CdO thin films obtained by sol gel method, *Thin Solid Films.*, 371, 105-108 (2000).
- [13] H.Khallaf, C.T. Chen, L.B. Chang, O.Lupan, A.Dutta, H. Heinrich, A. Shenouda, and L Chow. Investigation of chemical bath deposition of CdO thin films using three different complexing agents. *Applied Surface Science*, 257, 9237–9242 (2011).
- [14] E. Aydin, N. Demirci Sankir. AZO/metal/AZO transparent conductive oxide thin films for spray pyrolyzed copper indium sulfide based solar cells. *Thin Solid Films.*, 653, 29–36 (2018).
- [15] P. Sakthivel, S. Asaithambi, M. Karuppaiah, M. et al. Different rare earth (Sm, La, Nd) doped magnetron sputtered CdO thin films for optoelectronic applications. *J Mater Sci: Mater Electron.*, 30, 9999–10012 (2019).
- [16] R.K. Gupta, Z. Serbeti, F. Yakuphanoglu. Bandgap variation in size controlled nanostructured Li-Ni co-doped CdO thin films. *Journal of Alloys and Compounds.*, 515, 96–100 (2012).
- [17] P. Velusamy, R. Ramesh Babu, K. Ramamurthi, E. Elangovan, J. Viegas, M.S Dahlem, and M. Arivanandhan. Characterization of spray pyrolytically deposited high mobility praseodymium doped CdO thin films. *Ceramics International.*, 42, 12675–12685 (2016).

- [18] M.R. Alam, M. Mozibur Rahman, A.M.M Tanveer Karim, and M.K.R. Khan. Effect of Ag incorporation on structural and opto-electric properties of pyrolyzed CdO thin films. *Int Nano Lett.*, **8**, 287–295 (2018).
- [19] R.J. Deokate, S.M. Pawar, A.V. Moholkar, V.S. Sawant, C.A. Pawar, C.H. Bhosale, and K.Y. Rajpure. Spray deposition of highly transparent fluorine doped cadmium oxide thin films. *Applied Surface Science.*, **254**, 2187–2195 (2008).
- [20] Bong Ju Lee, Jin Jeong. A Study of Structural and Photoluminescence for Al-Doped CdO Thin Films. *Journal of Spectroscopy.*, 1-7 (2016).
- [21] Ravikumar, M., Chandramohan, R., Kumar, K.D.A. Effect of Nd doping on structural and opto-electronic properties of CdO thin films fabricated by a perfume atomizer spray method. *Bull Mater Sci.*, **42**, 1-8 (2019).
- [22] Azizar Rahman M, Khan M K R. Effect of annealing temperature on structural, electrical and optical properties of spray pyrolytic nanocrystalline CdO thin films. *Materials Science in Semiconductor Processing.*, **24**, 26–33 (2014).
- [23] Aydemir S, Köse S, Selami Kilickaya M, Özkan V. Influence of Al-doping on microstructure and optical properties of sol-gel derived CdO thin films. *Superlattices and Microstructures.*, 71–81 (2014).
- [24] Akyuz I, Kose S, Ketenci E, Bilgin V, Atay F. Optical, structural and surface characterization of ultrasonically sprayed CdO:F films. *Journal of Alloys and Compounds.*, **509(5)**, 1947–1952 (2011).
- [25] Abdolazadeh Ziabari A, Ghodsi F E, Kiriakidis G. Correlation between morphology and electro-optical properties of nanostructured CdO thin films: Influence of Al doping. *Surface and Coatings Technology.*, **213**, 15–20 (2012).
- [26] Ahmed H. H. Variation of the structural, optical and electrical properties of CBD CdO with processing temperature. *Materials Science in Semiconductor Processing.*, **66**, 215–222 (2017).
- [27] Domenico A. Cristaldi, Salvatrice Millesi, Isodiana Crupi, Giuliana Impellizzeri, Francesco Priolo, Robert M. J. Jacobs, Russell G. Egdell, and Antonino Gulino. 2014, Structural, Electronic, and Electrical Properties of an Undoped n-Type CdO Thin Film with High Electron Concentration. *The Journal of Physical Chemistry C.*, **118(27)**, 15019-15026 (2014).
- [28]. Dakhel A. A. Transparent conducting properties of samarium-doped CdO. *Journal of Alloys and Compounds.*, **475(1–2)**, 51–54 (2009).
- [29]. Ravikumar M, Ganesh V, Shkir M, Chandramohan R, Arun Kumar K D. Fabrication of Eu doped CdO [Al/Eu-nCdO/p-Si/Al] photodiodes by perfume atomizer based spray technique for opto-electronic applications. *Journal of Molecular Structure.*, **1160**, 311–318 (2018).
- [30] Yahia I S, Salem G F, Abd El-Sadek M S, Yakuphanoglu F. Optical properties of Al-CdO nanoclusters thin films. *Superlattices and Microstructures.*, **64**, 178–184 (2013).
- [31] Velusamy P, Babu R Ramesh, - Ramamurthi K, Dahlem N. Sadeq et al: Preparation and study of properties of ... M S, Elangovan E. Highly transparent conducting cerium incorporated CdO thin films deposited by a spray pyrolytic technique. *RSC Adv.*, **5**, 102741-102749 (2015).
- [32] Helen S J, Devadason S, Mahalingam T. Improved physical properties of spray pyrolysed Al: CdO nanocrystalline thin films. *J Mater Sci: Mater Electron.*, **27**, 4426–4432 (2016).
- [33] Al-Ghamdi A A, Al-Hartomy O A, El Okr M, Nawar A M, El-Gazzar S, El-Tantawy F, Yakuphanoglu F. Semiconducting properties of Al doped ZnO thin films. *Spectrochimica Acta - Part A: Molecular and Biomolecular Spectroscopy.*, **131**, 512–517 (2014).
- [34] Murali K R, Kalaivanan A, Perumal S, Pillai N N. Sol-gel dip coated CdO: Al films. *Journal of Alloys and Compounds.*, **503(2)**, 350–353 (2010).
- [35] Wongcharoen N, Gaewdang T, Wongcharoen T. Electrical properties of Al-doped CdO thin films prepared by thermal evaporation in vacuum. *In Energy Procedia.*, **15**, 361–370 (2012).